Manuscript

A Hybrid Method for Calculating Residual Stress and Deformation in Space Hardware on Earth

Michael T. Britz
Graduate Student
Department of Mechanical and Aerospace Engineering
University of Alabama in Huntsville
Huntsville, AL 35899
Phone: (256) 426-7414; Email: britzm@uah.edu

John A. Gilbert
Professor of Mechanical Engineering
Department of Mechanical and Aerospace Engineering
University of Alabama in Huntsville
Huntsville, AL 35899
Phone: (256) 824-6029; Email: jag@eng.uah.edu

Teng K. Ooi
Adjunct Associate Professor
Department of Mechanical and Aerospace Engineering
University of Alabama in Huntsville
Huntsville, AL 35899
Phone: (256) 450-2869; Email: teng.ooi@mda.mil

Abstract

Many times in testing space hardware it is desirable to quantify residual von Mises stresses and deformation in a test article which will ultimately be placed in a micro-gravity environment. When testing in a 1-g environment the stresses and deformations include the contributions due to weight. This investigation demonstrates a hybrid method used to identify the residual von Mises and deformations that reflect a no weight condition. To this end, an example of a hard X-ray space mirror is presented to demonstrate this hybrid method which combines finite element analysis with experimental profile measurements, made under gravity loading, on a prototype formed by electroforming a thin shell on a cylindrical aluminum mandrel.

Keywords

Residual stress, finite element analysis, hybrid method

Introduction

To illustrate a hybrid method of calculating residual stresses in an article of space hardware an example of a hard x-ray mirror is considered. Direct determination of residual stress can be made with several methods, for instance, indentation (Suresh and Giannakopoulos 1998) but can be costly and time-consuming. However, a simple and less expensive approach may be used for early design purposes. An example of this procedure, using an x-ray mirror is described below.

RETRACTED

. The Constellation-X Observatory was a mission concept for an X-ray space observatory to be operated by NASA. The objective was to investigate black holes, Einstein's Theory of General Relativity, galaxy formation, the evolution of the Universe on the largest scales, the recycling of matter and energy, and the nature of "dark matter."

The telescope aboard the satellite was designed to operate in the ~40 keV portion of the electromagnetic spectrum and, as illustrated in Fig. 1, relied on an array of primary mirrors nested within each other. The mirrors follow mathematical curves - the parabola and hyperbola - derived by slicing through an imaginary cone at different angles.

X-ray telescopes are very different from optical telescopes, because with their high energies, X-ray photons will simply pass through a conventional mirror. To solve this problem, the mirrors are cylindrically-shaped so that hard X-rays (~ 40 keV) are deflected into the instrument like stones skipping off water.

In a Wolter-I design (Wolter 1952), incoming photons undergo two reflections, the first from a parabolic surface and the second from a hyperbolic surface, to give an image that is essentially coma free. One approach developed to construct this design is to produce full-shell, shallow-graze-angle, gold-coated replicated mirrors by using electroformed nickel replication (Ramsey et al 1999, Ramsey et al 2000).

The advantage of electroforming is that complex coating procedures are avoided. The process lends itself readily to the multiple-mirror-module approach that small graze angles necessitate and the resulting shells provide excellent angular resolution that results in high sensitivity observations. This in turn translates directly into greater sensitivity through reduced focal spot size. Finally, with the use of high strength alloys one can achieve the stringent weight requirements of space-based missions.

During the mirror fabrication process, nickel mirror shells are electroformed onto a figured and highly polished aluminum mandrel from which they are later released by differential thermal contraction. Figure 2 illustrates that the resulting mirror shells are full circles of revolution.

The axisymmetric geometry provides good structural stability permitting good figure accuracy, and hence very good angular resolution. Since nickel has a high density, researchers must make very thin shells to achieve the lightweight optics necessary to keep launch costs reasonable.

The shells must be strong enough to withstand the stresses of fabrication and subsequent handling without undergoing permanent deformation. They must also be electroformed in an ultra-low-stress environment

RETRACTED

RETRACTED

to prevent stress-induced distortions once they are released. In short, the challenge is to maintain high angular resolution despite small weight-budget-driven mirror shell thickness. These requirements make shells extremely sensitive to the fabrication process and handling stresses.

The current mandrels used for electroforming represent conical approximations to Wolter-I geometry and typical metrology gives a performance prediction for the shells of around 8- to 10-arcsec half-power diameter (HPD), meaning half the reflected flux from a point source falls within this angular range. However, X-ray tests reveal shell performances in the 13- to 15-arcsec range with modules running around 17-arcsec HPD (Ramsey et al 2000, Ramsey et al 2002). Consequently, it is essential to identify the source and extent of these discrepancies so that steps can be taken to correct them.

In a recent study (Franco 2003), laser techniques were applied to profile an electroplated shell after it was manufactured. When the shell was positioned vertically on a flat surface under laboratory conditions, profile measurements revealed that distortions in the mirrored surface created excessive optical distortion in the telescopic system. It was hypothesized that anomalies in the shape of the shell were due to residual stresses developed either during the electroplating process or while the shell was thermally removed from its mandrel. The removal process was eliminated as a source for these anamolies by further research (Franco et al 2005).

Hybrid Analysis

The hybrid approach consists of determining the von Mises stress due to electroplating by subtracting the stress on the shell created by a gravity loading from the total stress computed based on profile measurements. Simply put,

$$\sigma_{RESIDUAL} = \sigma_{EXPERIMENTAL} - \sigma_{GRAVITY} \qquad (1)$$

The residual deformations are obtained in a similar manner by subtracting the deformation due to gravity from the deformation computed based on profile measurements. Again,

$$\delta_{RESIDUAL} = \delta_{EXPERIMENTAL} - \delta_{GRAVITY} \qquad (2)$$

Conical Shell Manufacturing Process

Figure 3 shows the test article developed for this study. As illustrated in the schematic on the left, the mirror is 58.42 cm (23 in.) long and consists of an ultra thin shell that is slightly conical in shape. One half of the test article has a parabolic shape and an outer edge radius of 24.69 cm (9.72 in.) whereas the other half is hyperbolic with an edge radius of 24.66 cm (9.707 in.). Since the inner surface serves as a mirror for high resolution optical imaging, the shape of the shell must be carefully controlled during the manufacturing process. A cross section of the five layers of interest and their thicknesses for the case considered are shown to the right in Fig. 3.

The production of the mirror involves several steps. The first step is the fabrication of an aluminum mandrel with a radius of 0.102 mm (0.004 in.) below that required for the shell. Next, the mandrel is coated with 0.099 mm (0.0039 in.) of electroless nickel to give a hard surface suitable for polishing. Then the mandrel is accurately figured using a cylindrical grinding machine. Finally, a mechanical super polishing takes place, sufficient to ensure that scattering does not dominate the mirror's performance up to the cut-off energy.

To prepare for electroforming, the surface of the mandrel is treated to form an oxide layer from which the shell can be easily released. Then the mandrel is immersed in the plating tank. A typical shell takes approximately 1 day to electroform, at which time the plated mandrel is taken from the bath, rinsed, and dried. Then the assembly is cooled to separate the shell from the mandrel. This is accomplished by immersing it into a dewar of liquid nitrogen and then sliding the mandrel from the shell as release takes place. The process relies on the differences in the thermal coefficients of expansion of the materials and the relative bond strength between the layers to separate the top two layers from the mandrel. The final configuration consists of an ultra thin, open ended, conical shell, with a gold mirror on the inside and a cobalt-nickel substrate on the outside.

Experimental Measurements

A series of experimental tests were conducted to support this work including thickness measurement, profiling, and yield stress determination. The shell was positioned vertically and profile measurements were taken on the outer surfaces along four meridians: 0, 90, 180, and 270 degrees. An average thickness of 0.333 mm

RETRACTED

RETRACTED

(0.0131 in.) was used in the finite element model to take into account the variations in thickness over the height. Thickness values ranged from 0.33 mm (0.0130 in.) to 0.34 mm (0.0134 in.).

The shell profiles were measured in two separate runs (Gubarev et al 2001). The parabolic section was profiled first. Then the shell was inverted and the hyperbolic section profiled.

Figures 4 and 5 show the deviation of each of the meridians from the design geometry in the parabolic (top) and hyperbolic (bottom) sections, respectively. In each case, the shell was supported at a height of zero [0.0 mm (0.0 in.)]. If the shell contour were perfect, the curves would fall along the absissa. However, the plots show that the surface bulges outward along all of the meridians.

In the case of the parabolic section, a maximum deformation equal to 0.0089 mm (352 x 10^{-6} in.) occurs at 10.24 cm (4.03 in.) from the bottom in the 0 deg meridian. Three local maxima are observed on the curves and the deformation decreases to zero at a height of 29.21 cm (11.5 in.), corresponding to the mid-section of the shell.

In the case of hyperbolic section, the shell bulges outward and a maximum deformation equal to .0067 mm (262 μ in.) occurs at 1.57 mm (0.62 in.) from the bottom in the 180 deg meridian. Six local maxima are observed and the deformation decreases to zero at the mid-section, corresponding to a height of 29.21 cm (11.5 in.).

Finite Element Analysis

The finite element model (FEM) used to analyze the shell was generated by using MSC/Nastran. See Fig. 6. Since the mirror is a shell, the model was meshed using 4-node quadrilateral (CQUAD4) elements. A total of 18480 elements and 18720 nodes were generated. The cobalt-nickel substrate was assumed to be linearly elastic, homogeneous, and isotropic with properties obtained from the tensile test. A convergence test consisting of doubling the mesh density to ascertain any change in results was conducted. It was concluded that the existing mesh was adequate.

Two load cases were analyzed while assuming that a gravity load was applied: the first with the average readings taken during profiling imposed along the meridians; the second with the shell subjected to gravity only.

In both cases the shell was assumed to be supported along the bottom edge at 12 equally spaced points. The tangential and longitudinal components were constrained at the supports while the radial and all rotation components remained free.

Hybrid Results

Equations 1 and 2 were applied to obtain the von Mises stress and radial deformation under microgravity conditions. Figure 7 shows the residual stress plotted along a meridian for the parabolic (left) and hyperbolic (right) sections. Figure 8 shows the results obtained for the residual radial deformation.

The stress and deformation are radially symmetric and, as illustrated in Figs. 9, 10 and 11, can be depicted three-dimensionally in the form of Patran plots. The maximum stresses and deformations for the two sections of the model are summarized in Table 1.

Discussion

As mentioned previously, any deviations from the desired profile (see Fig. 7) that result from unwanted residual stress (see Fig. 8) produce abberations that reduce the overall optical performance of the device. Knowing the magnitude and distribution of these quantities will help designers make improvements.

A stress approach could be taken where the shell was purposefully deformed after fabrication to induce a permanent deformation equal and opposite to the deviation. However, this would require the shell to be ductile; unfortunately, this is not the case at present. An alternate approach would be to reconfigure the mandrel by undercutting it to account for the unwanted deformation.

Conclusion

The residual stress and deformation of a hard X–ray mirror under microgravity conditions can be determined with the use of a hybrid method. By subtracting the results obtained from a 1-g gravity loading from those derived experimentally from imposed deformation measured under laboratory conditions, the residual stress

RETRACTED

and deformation from the manufacturing process can be quantified. This technique could be used in a myriad of space test articles and satellites. Further work needs to be done, specifically the deformation of a test article in an actual 0-g enviroment needs to be ascertained and compared to the theoretical predictions.

Acknowledgement

The authors would like to thank the National Aeronautics and Space Administration at Marshall Space Flight Center in Huntsville, AL for providing the test data.

RETRACTED

References

Franco, J.E. (2003) "A combined analytical and experimental approach to the determination of residual stresses in very thin cylindrical shells" University of Alabama In Huntsville, Ph.D Dissertation, Mechanical and Aerospace Engineering.

Franco, J.E., Bower, M.V., Ooi, T.K., and Gilbert, J.A. (2005) "Hybrid stress analysis of an ultra-thin conical shell" *Proc. of SEM Annual Conference & Exposition on Experimental and Applied Mechanics*, Portland, Oregon, June 7-9, Paper No. 219, 10 pages.

Gubarev M.V., Kester T., and Takacs, P.Z. (2001) "Calibration of a vertical-scan long trace profiler at MSFC" *Proc. SPIE* Vol. 4451, pp. 333-339, Optical Manufacturing and Testing IV, Stahl, H. P., Ed., pp. 333-339.

Ramsey, B.D., Engelhaupt, D.E., Speegle, C.O., O'Dell, S.L., Austin, R.A., Kolodziejczak, J.J., and Weisskopf, M.C. (1999) "HERO program:high-energy replicated optics for a hard-x-ray balloon payload". *Proc. SPIE* Vol. 3765, EUV, X-Ray, and Gamma-Ray Instrumentation for Astronomy X, Siegmund, O.H., Flanagan, K.A., Eds., pp. 816-821.

Ramsey, B.D., Alexander, C.D., Apple, J.A., Austin, R.A., Benson, C.M., Dietz, K.L., Elsner, R.F., Engelhaupt, D.E., Kolodziejczak, J.J., O'Dell, S.L., Speegle, C.O., Swartz, D.A., Weisskopf, and M.C., Zirnstein, G. (2000) "HERO: high-energy replicated optics for a hard-x-ray balloon payload" *Proc. SPIE* Vol. 4138, X-Ray Optics, Instruments, and Missions IV, Hoover, R. B., Walker; A. B., Eds., pp. 147-153.

Ramsey, B.D., Alexander, C.D., Apple, J.A., Benson, C.M., Dietz, K. L., Elsner, R.F., Engelhaupt, D.E., Ghosh, K.K., Kolodziejczak, J.J., O'Dell, S.L., Speegle, C.O., Swartz, D.A., and Weisskopf, M.C. (2002) "First images from HERO, a hard x-ray focusing telescope" *The Astrophysical Journal*, Volume 568, part 1, page 432.

Suresh, S., and Giannakopoulos, E. (1998) "A new method for estimating residual stresses by instrumented sharp indentation" *Acta Metallurgica* Vol. 46 No. 16 pp. 5755-5767.

Wolter, H. (1952) Annalen der Physik 10.

RETRACTED

Section	von Mises Stress	Radial Deformation
Hyperbolic	4.56 MPa (662 psi)	0.0065 mm (2.54 x 10^{-4} in.)
Parabolic	5.32 MPa (772 psi)	0.0091 mm (3.58 x 10^{-4} in.)

Table 1 FEM results for maximum residual stress and radial deformation

RETRACTED

Figure

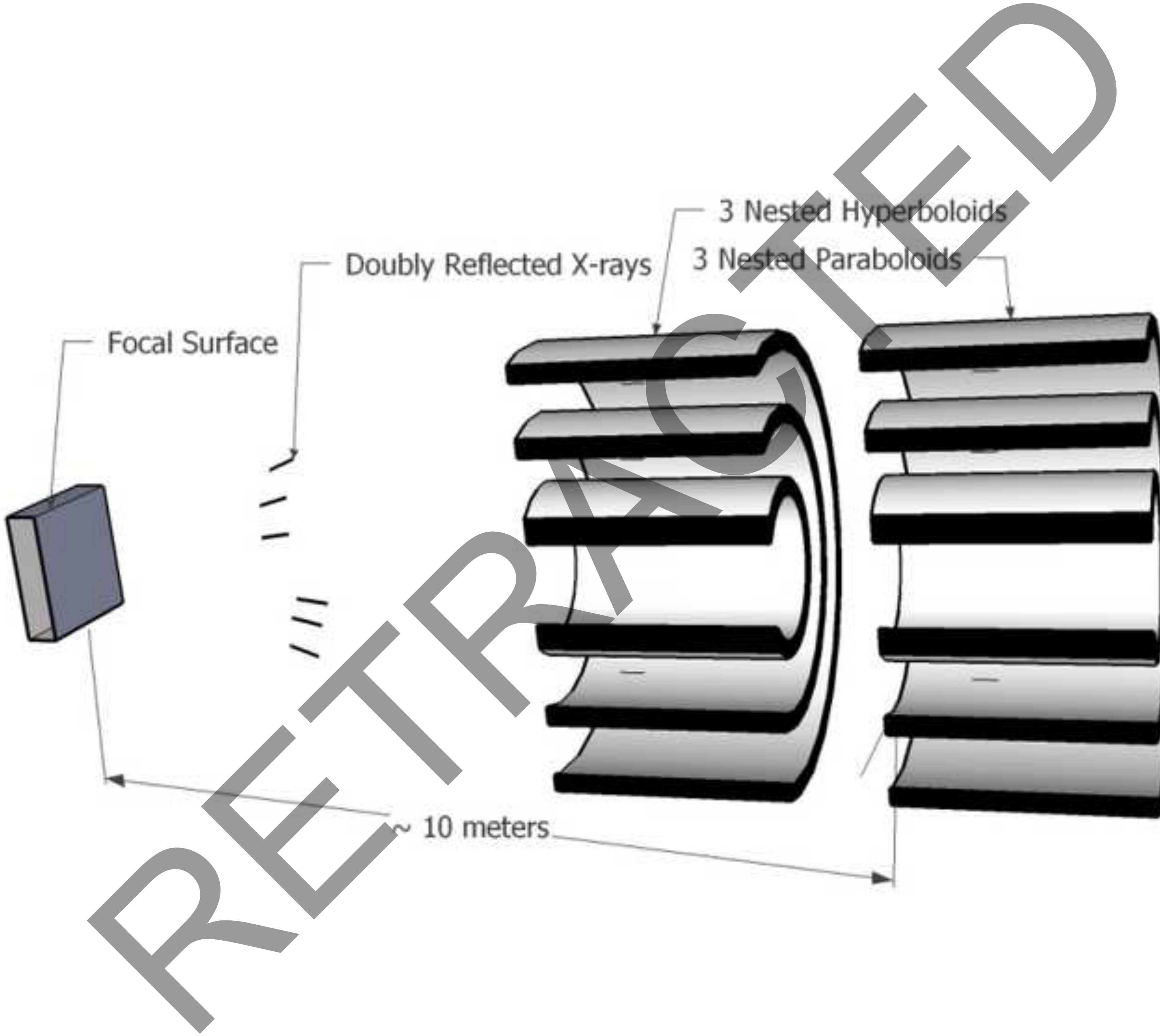
3 Nested Hyperboloids
Doubly Reflected X-rays
3 Nested Paraboloids
Focal Surface
~ 10 meters
RETRACTED

Figure

RETRACTED

Figure

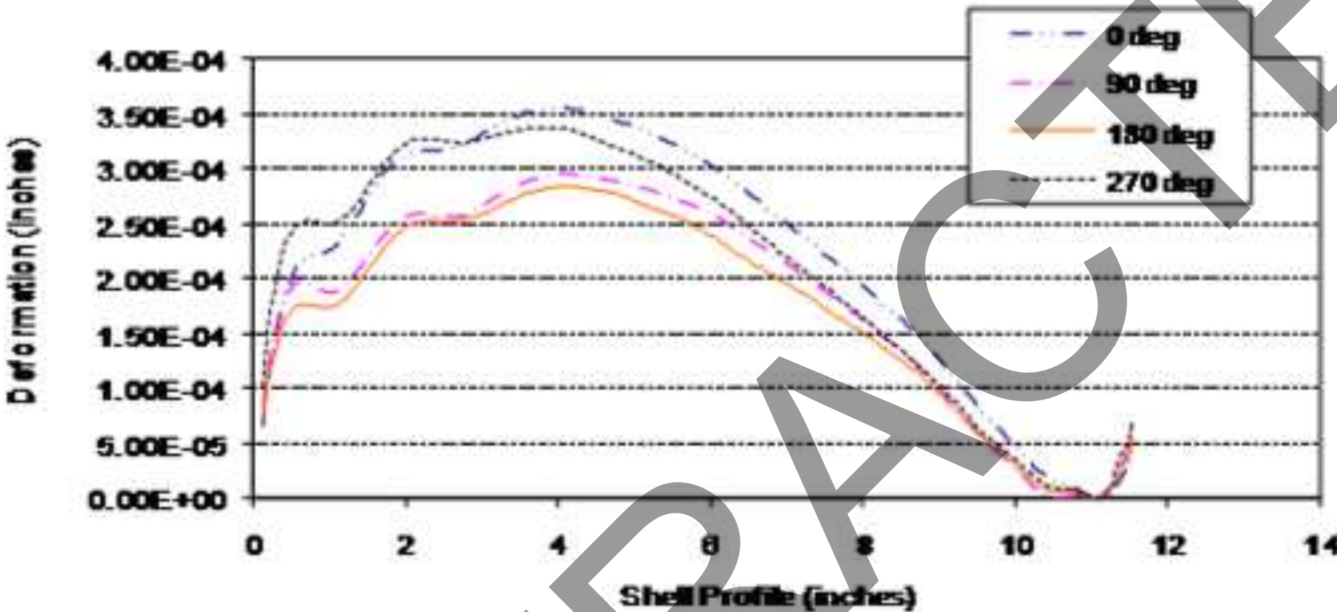

RETRACTED

Figure

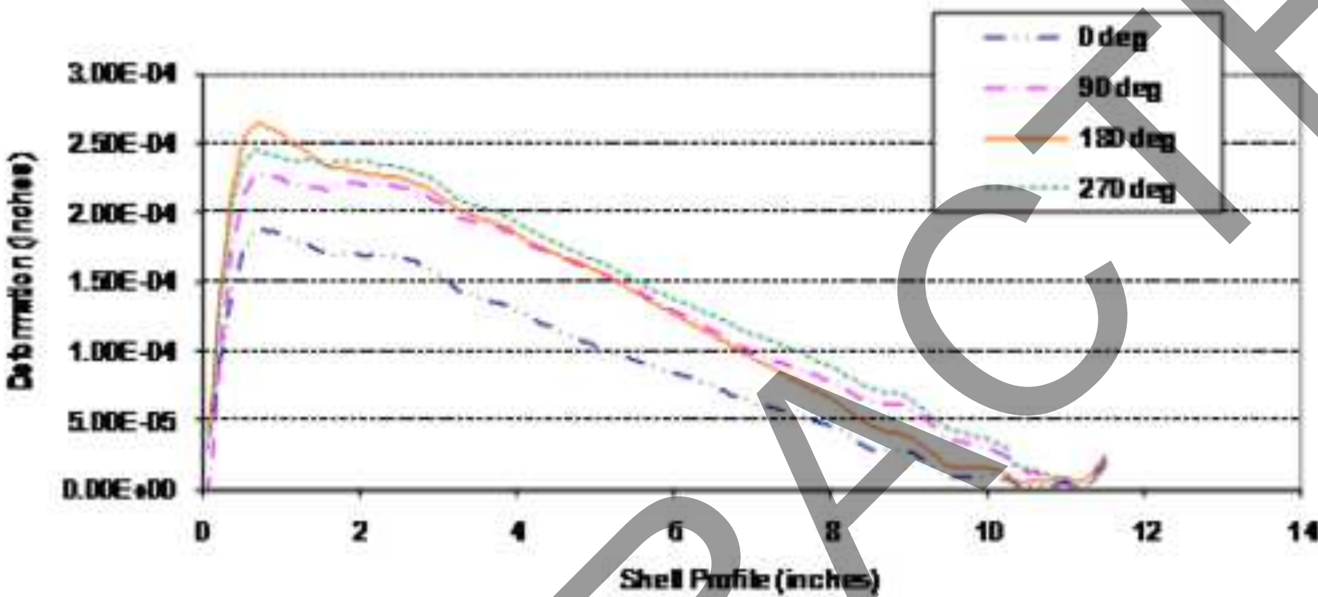

RETRACTED

Figure

RETRACTED

Figure

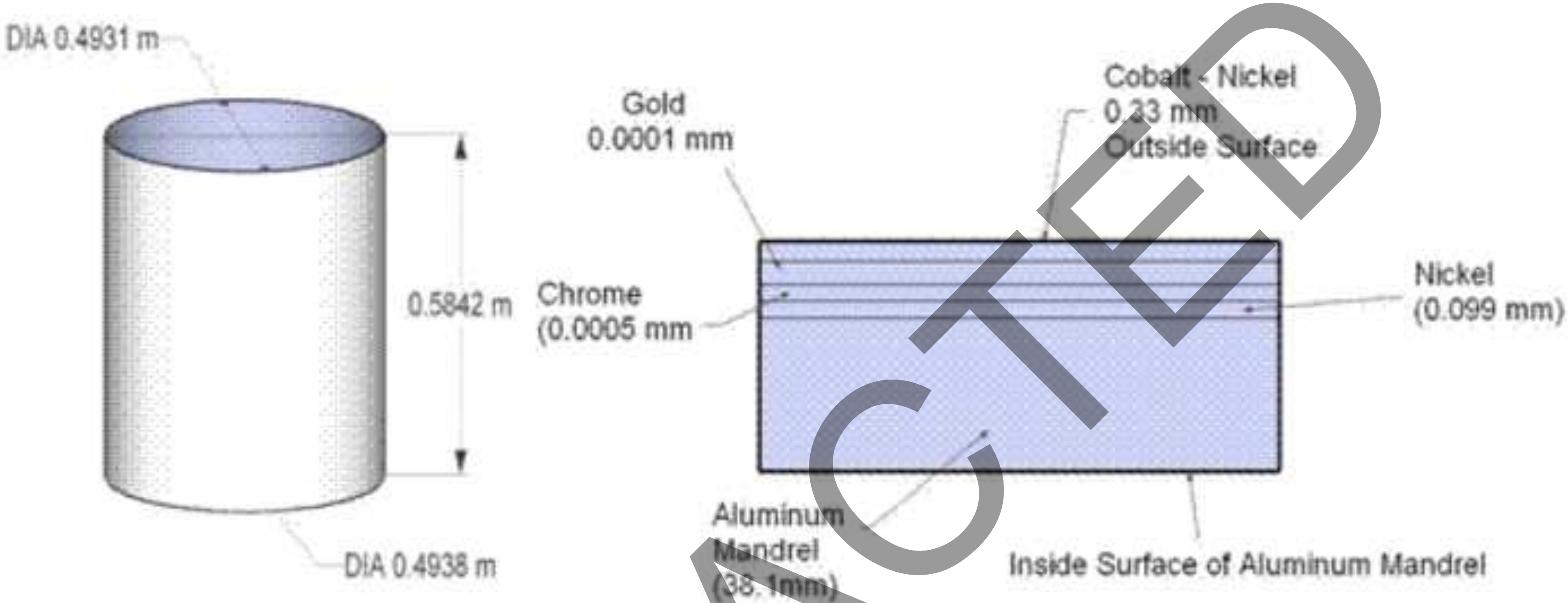

RETRACTED

Figure

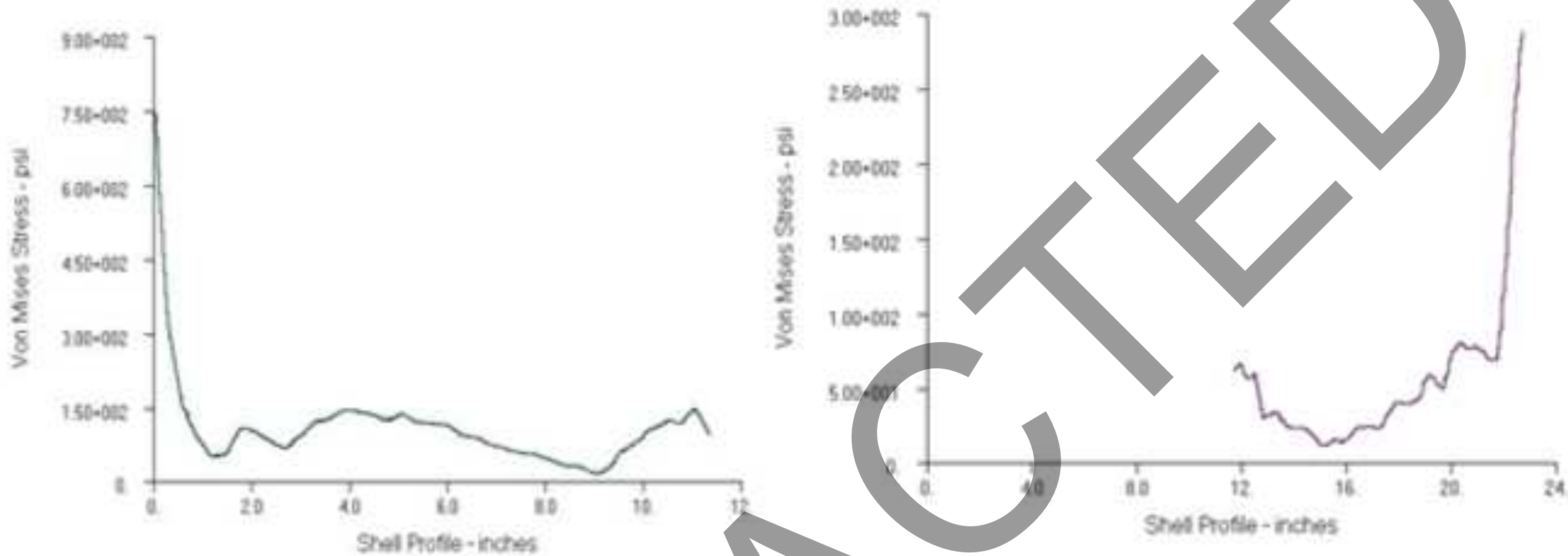

RETRACTED

Figure

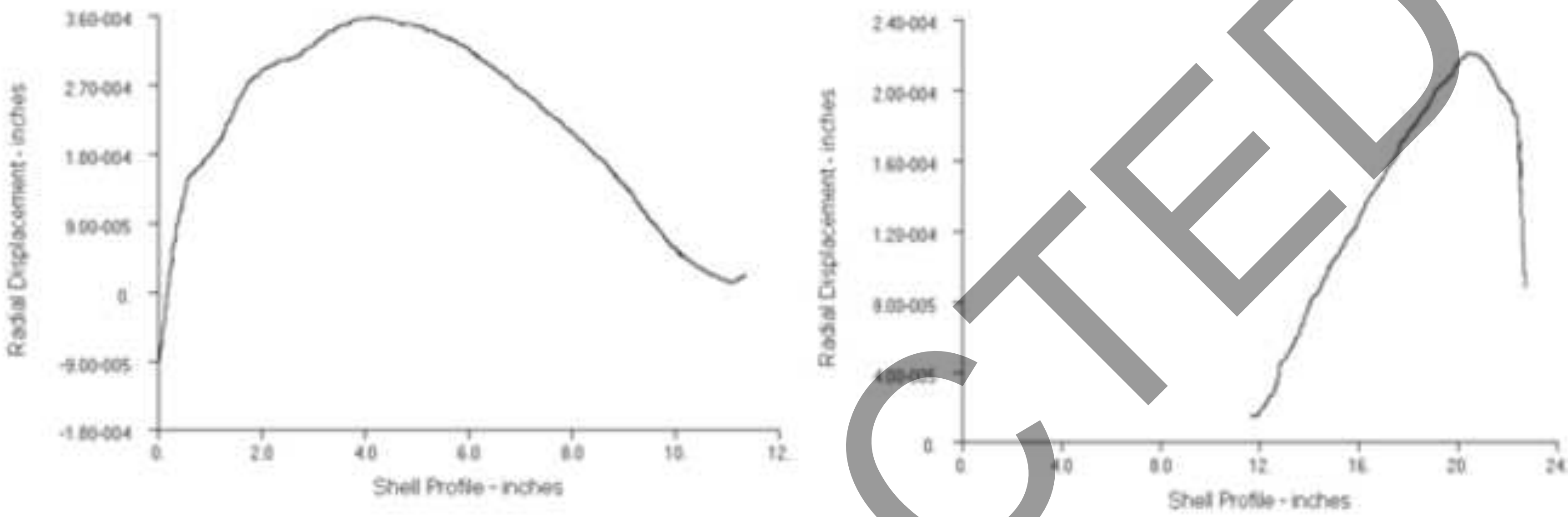

RETRACTED

Figure

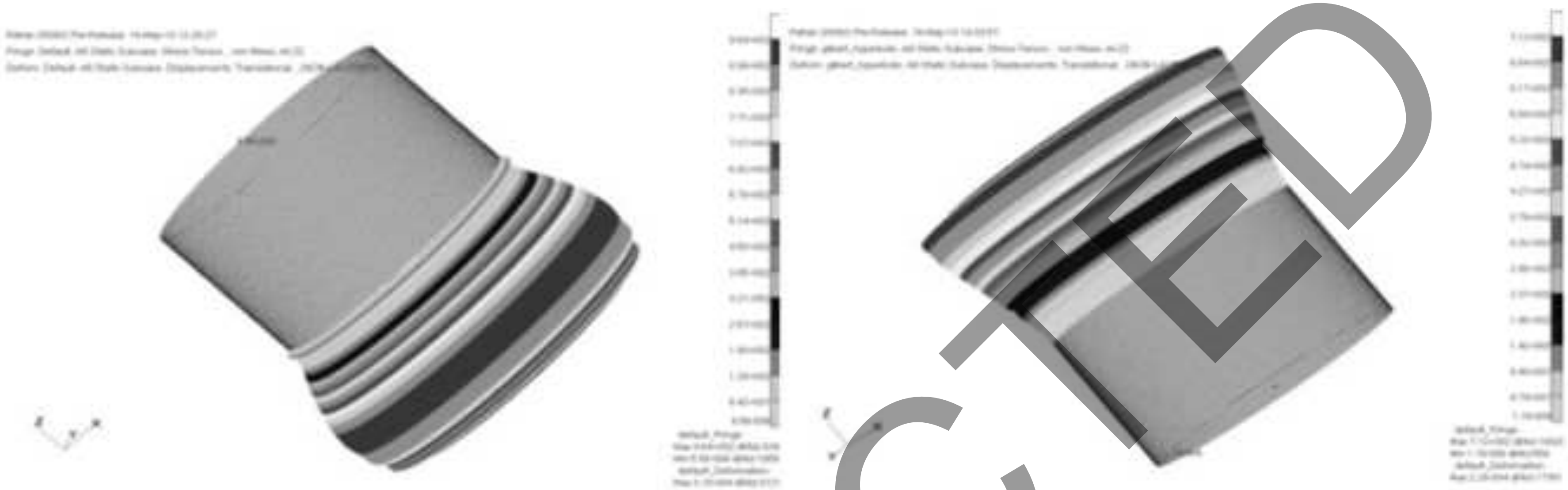

RETRACTED

Figure

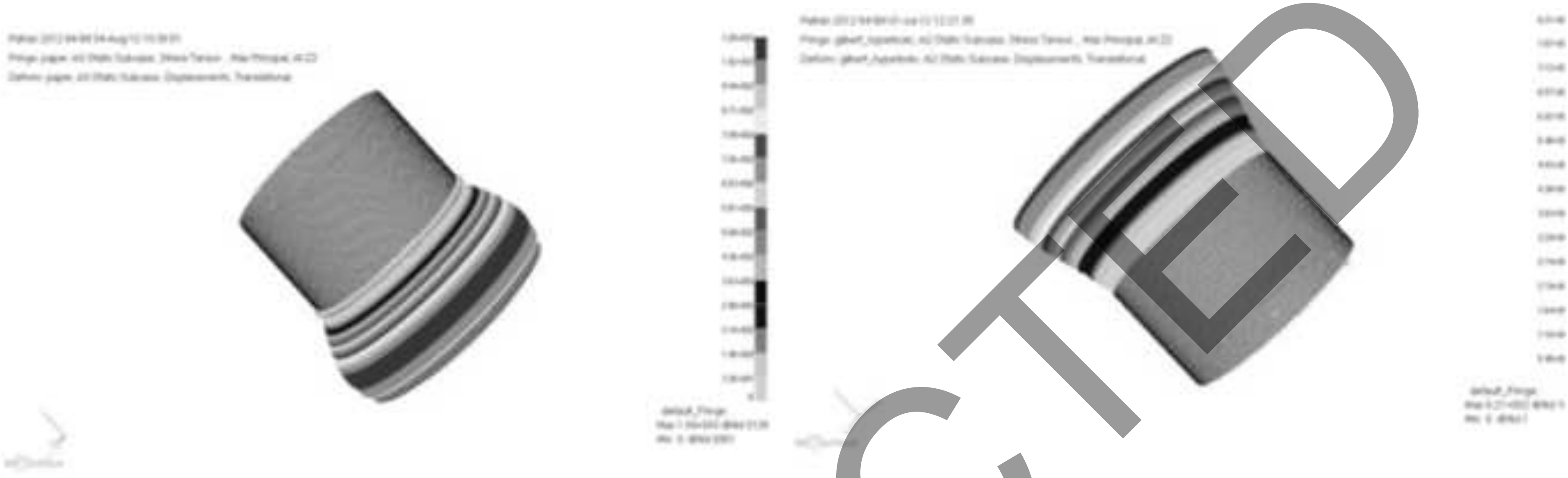

RETRACTED

Figure

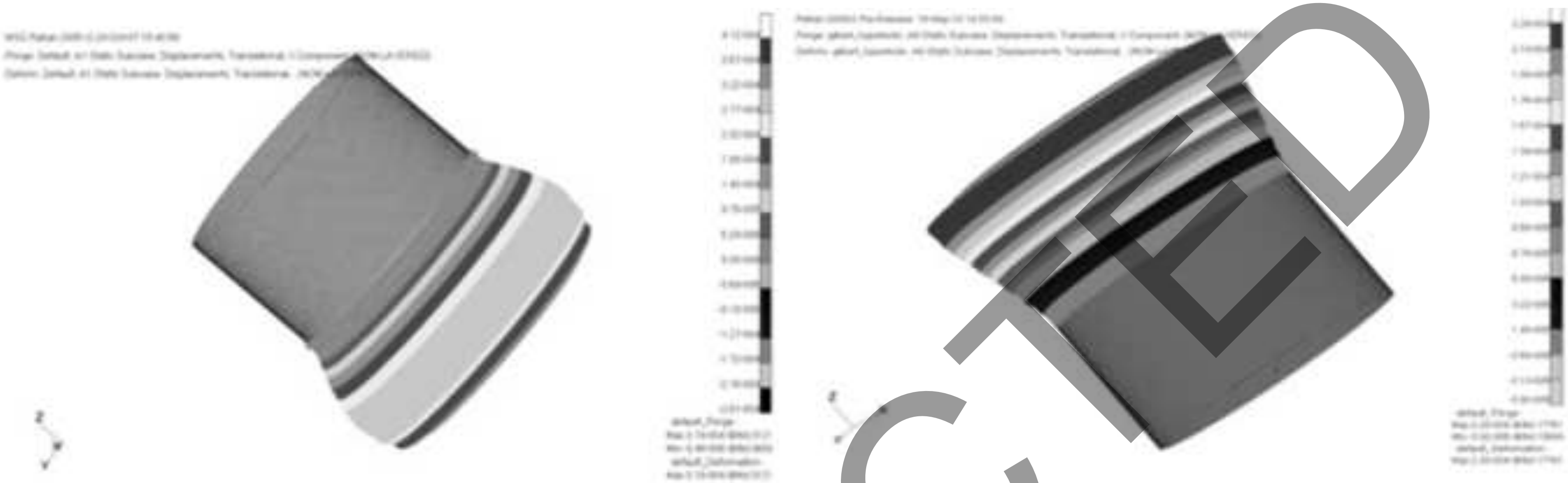

RETRACTED

FIGURE 1 The optical train and mirror cross section of a typical X-ray space telescope.

FIGURE 2 A thin shell mirror mounted in a support ring. Photo by Carl Benson, NASA/MSFC

FIGURE 3 Shell dimensions (left) and mirror cross section (right)

FIGURE 4 Parabolic shell profiles along four meridans

FIGURE 5 Hyperbolic shell profiles along four meridians

FIGURE 6 Finite Element Model

FIGURE 7 Residual von Mises stress plotted along a meridian for the parabolic (left) and hyperbolic (right) sections

FIGURE 8 Residual radial deformation plotted along a meridian for the parabolic (left) and hyperbolic (right) sections

FIGURE 9 Residual von Mises stress in the parabolic (left) and hyperbolic (right) sections

FIGURE 10 Residual Max Principal Stress in the parabolic (left) and hyperbolic (right) sections

FIGURE 11 Residual radial deformation in the parabolic (left) and hyperbolic (right) sections

RETRACTED